COSMIC RAYS UNDERGROUND

By B. V. Srikantan and S. Naranan
(*Tata Institute of Fundamental Research, Bombay-1*)

Received May 12, 1952
(Communicated by Prof. H. J. Bhabha, F.A.SC., F.R.S.)

During the months of October, November and December, 1951, an investigation on cosmic-ray intensity was carried out in the Gold Mines at Kolar (Mysore State) surface altitude 2,800 ft., with a hodoscoped counter telescope, upto a depth of 1,008 meters water equivalent. The experimental details, and the main results of the investigation are presented in this paper under the following Sections:—

Section I. Experimental details.
Section II. Intensity Measurements, vertical flux at various depths.
Section III. Angular Distribution of underground particles.
Section IV. Production of Secondaries by μ-mesons.
Section V. Deduction of the Energy Spectrum of π-mesons and of μ-mesons from the intensity measurements.
Section VI. Nature of the neutral radiation underground.
Section VII. Comparison of results with the results of other experiments and Discussion.

Section I. Experimental Details

The apparatus used is shown in Fig. 1. Six counters of length 37·5 cm. and diameter 4·0 cm. were placed in each of the trays A, B, C and D. The trays A and B were separated by a lead absorber 2·5 cm.

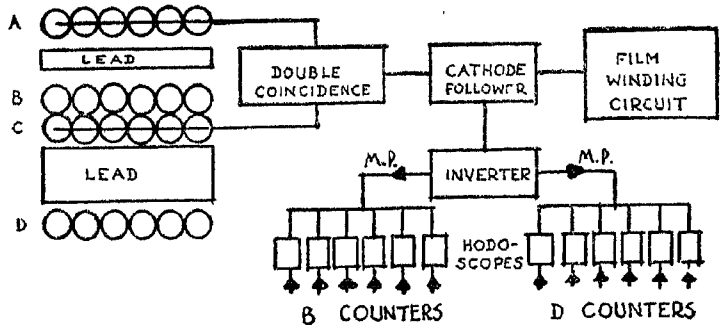

Fig. 1. Block Diagram Showing the Essential Electronic Circuits.

thick, and trays C and D by a lead absorber 7·5 cm. thick. The extreme trays A and D were separated by 27·5 cms. The semi-angles of acceptance of the telescope ABCD were 40° and 54° in the planes perpendicular and parallel to the counter axes. The semi-angles of ABC in the two planes were 60° and 68°. All the counters were filled with argon and petroleum ether in the ratio 9 : 1, to a total pressure of 10 cm. The counters were operated about 50 volts above the threshold voltage. The efficiency of the counters was found to be 98·5%.

The counters in trays B and D were hodoscoped with AC double coincidence pulse as the master triggering pulse.* A block-diagram showing the essential electronic circuits is given in Fig. 1. The circuit diagrams of the hodoscope and the film-winding circuit are given in Fig. 2 (*a*) and Fig. 2 (*b*). Each hodoscope plug-in unit consisted of a twin-triode (7F7)

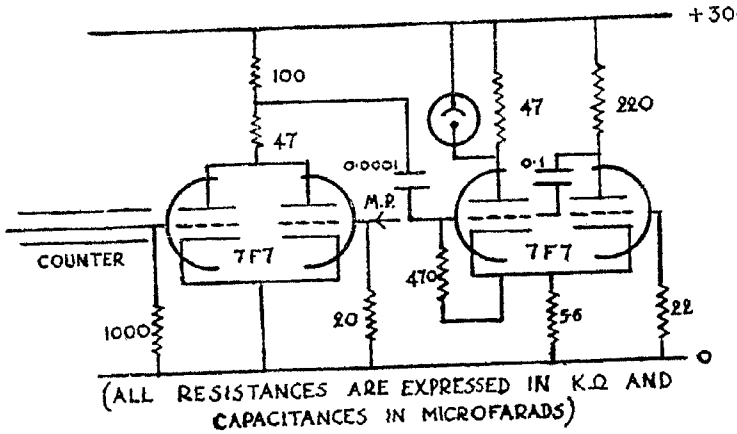

FIG. 2 (*a*). Hodoscope Circuit.

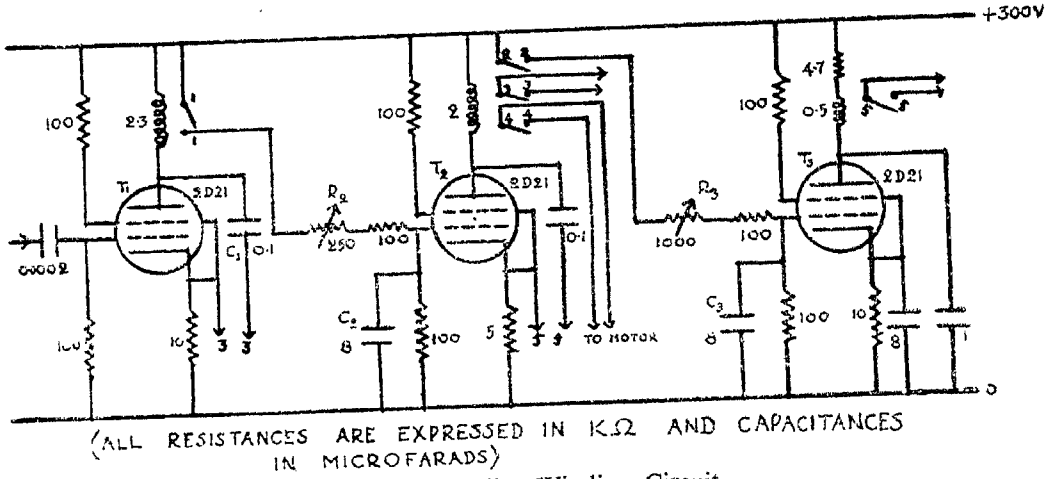

FIG. 2 (*b*). Film Winding Circuit.

* At 10 and 22 mwe, where the AC rate was too high for photography every thirty-second AC pulse was taken as the master pulse.

which selected coincidences of the AC master pulse, and the counter pulse; and a univibrator (7F7) to broaden the coincidence pulse for flashing a neon indicator. Since the plug-in units were placed close to the counter trays, it was not found necessary to use a pre-amplifier-cathode-follower-inverter system for every counter. For AC double coincidence, 6AK5 miniature pentodes were used. The coincidence pulse was fed to a 6J6 cathode-follower. Two outputs were taken from the cathode point of the cathode-follower. One output, after inversion, served as the master-pulse for all the coincidence stages of the hodoscopes. The second output was fed to the grid of the first thyratron of the film winding circuit.

Since the neon indicators connected in the plate of the univibrators flashed for a considerable time, it was essential to introduce a delay between the arrival of the master pulse on the grid of the first thyratron and the winding of the film. This was achieved by the thyratron delay circuit shown in Fig. 2, in the following way: With the arrival of the master pulse, the thyratron T_1 fired. It was not switched off immediately since the condenser C_1 was not connected to the cathode. A pair of off-to-on contacts of the relay in the plate of T_1 began charging the condenser C_2 in the grid of T_2 through the resistance R_2. As soon as the voltage on C_2 rose above the cut-off bias of T_2, the thyratron T_2 fired. T_2 too was not switched off immediately. The relay in the plate of T_2 had three pairs of off-to-on contacts. One pair switched off T_1 by connecting C_1 to the cathode of T_1. Another pair put on the D.C. voltage for the film-winding motor. The third pair started charging C_3 through R_3. As soon as the voltage on C_3 exceeded the cut-off bias of T_3, the thyratron fired, but was automatically switched off. The pair of contacts of the relay in the plate of T_3 switched off T_2. The delay time was controlled by C_2 and the potentiometer R_2, and the winding time of the motor by C_3 and the potentiometer R_3.

The experiment was first carried out at the surface. Then it was repeated at depths 503, 598, 807, 1008 mwe. The 22 mwe level was covered at the end. Though the main shaft was very wet, the places at which the experiment was set up, were comparatively free from moisture. Except at 1008 and 22 mwe, the telescope was more than 600 ft. away from the main shaft, at all depths. At 1008 mwe, it was 200 ft. away and at 22 mwe, about 10 ft. away from the shaft.

Section II. Intensity Measurements

From the hodoscope photographs, we were able to deduce the following counting rates:—

(i) the three-fold coincidence rate N_{ABC} (counts per hour) of particles capable of penetrating 2·5 cm. of lead, recorded by the telescope with semi-angles of acceptance 60° and 68° in the two planes;

(ii) the four-fold coincidence rate N_{ABCD} (counts per hour) of particles penetrating 10 cm. of lead, recorded by the telescope with semi-angles 40° and 54°;

(iii) the four-fold coincidence rate of particles penetrating 10 cm. lead, as recorded by a system of five single counter telescopes with semi-angles 12° and 64°.

Table I gives the recorded rates N_{ABC}, N_{ABCD} at various depths. They are plotted against depth expressed in mwe on a log-log scale in Fig. 3. The

TABLE I

Depth H mwe	$E_{min.}$ (Bev) of μ-mesons penetrating H mwe	N_{ABC} (counts per hr.)	N_{ABCD} (counts per hr)	I_{ABC}	I_{ABCD}	I_V	$\frac{I_{ABCD}}{I_{ABC}} \times 100$
10	2·966	21440±610	9414±410	$7{\cdot}42 \times 10^{-3}$	$5{\cdot}88 \times 10^{-3}$	$6{\cdot}11 \times 10^{-3} \pm 0{\cdot}49 \times 10^{-3}$	79·2
22	6·425	9215±272	3806±173	$3{\cdot}71 \times 10^{-3}$	$2{\cdot}67 \times 10^{-3}$	$2{\cdot}87 \times 10^{-3} \pm 0{\cdot}23 \times 10^{-3}$	72·0
503	152·8	54·3±2·6	25·6 ±1·8	$2{\cdot}56 \times 10^{-5}$	$2{\cdot}04 \times 10^{-5}$	$1{\cdot}76 \times 10^{-5} \pm 0{\cdot}24 \times 10^{-5}$	79·7
598	186·6	30·8±1·3	14·7 ±0·9	$1{\cdot}46 \times 10^{-5}$	$1{\cdot}19 \times 10^{-5}$	$1{\cdot}24 \times 10^{-5} \pm 0{\cdot}13 \times 10^{-5}$	81·5
807	269·5	11·4±0·6	5·3 ±0·4	$0{\cdot}539 \times 10^{-5}$	$0{\cdot}425 \times 10^{-5}$	$0{\cdot}555 \times 10^{-5} \pm 0{\cdot}070 \times 10^{-5}$	78·8
1008	370·6	4·74±0·21	2·33±0·15	$0{\cdot}224 \times 10^{-5}$	$0{\cdot}187 \times 10^{-5}$	$0{\cdot}237 \times 10^{-5} \pm 0{\cdot}027 \times 10^{-5}$	83·5

(The intensities I_{ABC}, I_{ABCD}, and I_V expressed in terms of particles cm.$^{-2}$ sec.$^{-1}$ sterad^{-1} have been computed using $\cos^2$ angular distribution for 10 mwe, $\cos^3$ distribution for 22 mwe, and $\cos^4$ distribution for 503–1008 mwe.)

last four experimental points corresponding to particles capable of penetrating 10 cm. lead, can be fitted to the straight line

$$\log_{10} N_{ABCD} = 10{\cdot}62 - 3{\cdot}41 \log_{10} H.$$

Similarly, the last four N_{ABC} rates, can be fitted to the straight line

$$\log_{10} N_{ABC} = 11{\cdot}30 - 3{\cdot}55 \log_{10} H.$$

These lead to the intensity-depth relations

$$N_{ABCD} = 10^{10{\cdot}62} H^{-3{\cdot}41 \pm 0{\cdot}01} \quad (1)$$

$$N_{ABC} = 10^{11{\cdot}30} H^{-3{\cdot}55 \pm 0{\cdot}06} \quad (2)$$

For the component penetrating 10 cm. of lead the slope of the line joining the surface point to the 22 mwe point is 1·15, and the corresponding

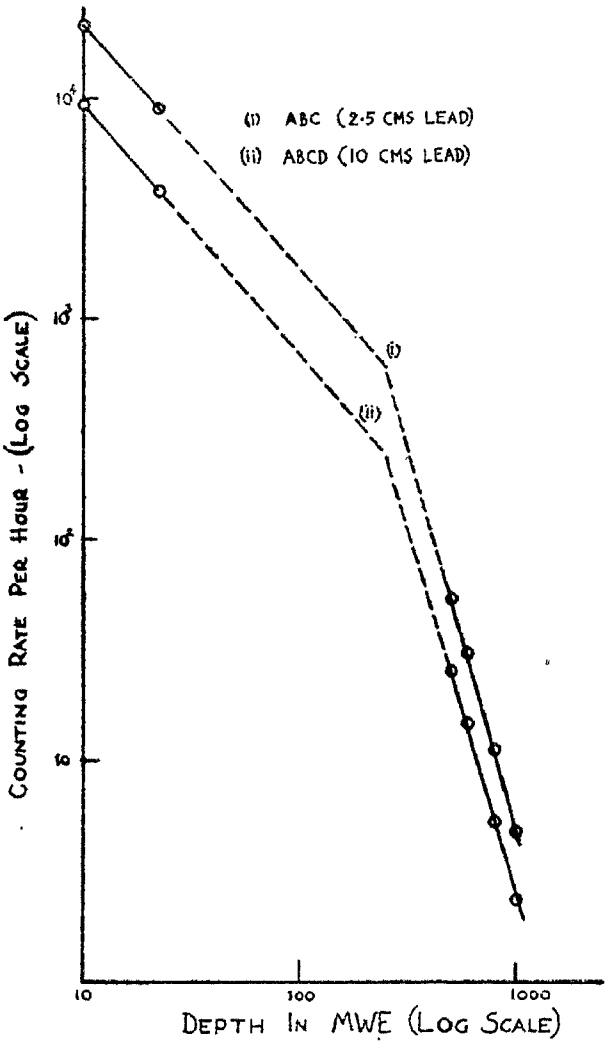

FIG. 3. Counting Rate—Depth Curves.

slope for radiation penetrating 2·5 cm. lead is 1·09. It is seen that for depths below 503 mwe, the absorption curves for the particles penetrating 2·5 and 10 cm. lead, run almost parallel. From the last column of Table I, it is seen that at all depths, nearly 80% of the particles penetrating 2·5 cm. lead are capable of penetrating 10 cm. lead.

Table I gives the flux values I_{ABC}, I_{ABCD}, and I_V, calculated from ABC, ABCD and the single-counter telescope counting rates, and also the ratio I_{ABCD}/I_{ABC}. The computations were made assuming $\cos^2$ angular distribution at 10 mwe, $\cos^3$ distribution at 22 mwe and $\cos^4$ distribution for depths 503–1008 mwe. The reasons for choosing these cosine powers are discussed in the following section (III). In the calculation of vertical flux, the angular distribution in both the planes was taken into account. The vertical flux I_V calculated from the single counter telescopes is more

accurate, since the effect of leakage spaces is a minimum. Between 500 and 1008 mwe the vertical intensities can be expressed by the power law,

$$I_V = 10^{3.56} H^{-3.1 \pm 0.1} \quad (3)$$

SECTION III. ANGULAR DISTRIBUTION OF UNDERGROUND PARTICLES

A detailed description of the procedure adopted for obtaining the angular distribution of underground particles, from the hodoscope records is given in the Appendix. The results are given in Fig. 4 and Fig. 5. The solid lines in the figures represent the distributions expected on the basis of $\cos^2$, $\cos^3$, and $\cos^4$ laws. The experimental points for the four angles 0°, 15½°, 29°, and 40° are also plotted in the same figures for the two depths 22 mwe and 598 mwe. It is seen that at 22 mwe, the experimental points are closer to the $\cos^3$ curve rather than $\cos^2$ or $\cos^4$ curves. But at 598 mwe, the experimental points are closer to the $\cos^4$ curve. While the number of particles recorded, particularly at large inclinations, is not sufficiently high for deciding unambiguously on the exact power law obeyed, the increasing steepness of the angular distribution curve with depth is unmistakable. However, it may be pointed out that in the computation of vertical flux, a change from $\cos^2$ to $\cos^3$ distribution increases the calculated flux by only 5%. The corresponding increase, when the distribution changes from $\cos^3$ to $\cos^4$ is 7%.

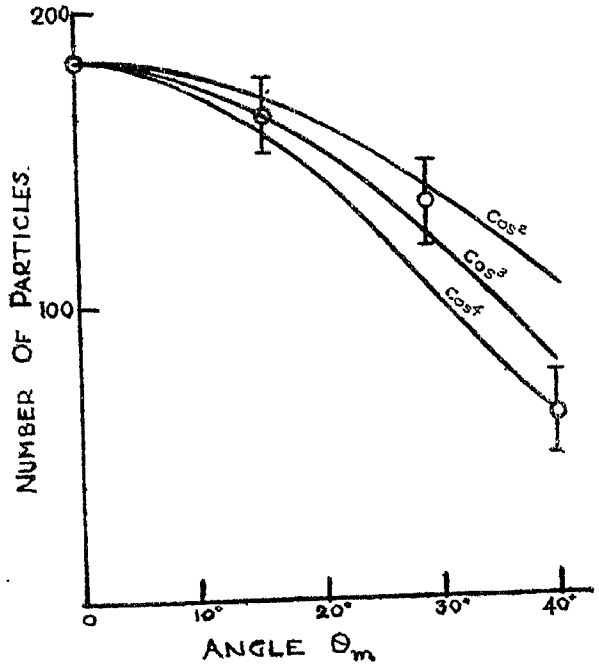

FIG. 4. Angular Distribution at 22 Mwe.

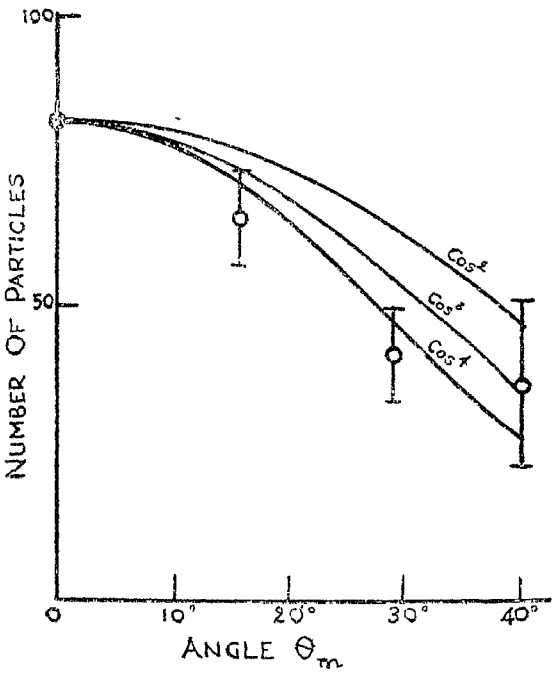

FIG. 5. Angular Distribution at 598 Mwe.

SECTION IV. PRODUCTION OF SECONDARIES BY μ-MESONS

(*A*) *Secondary production in the lead of the apparatus*

The experimental arrangement used for the measurement of intensity was suitable also for finding the percentage of μ-mesons that produced secondaries such as knock-on's, bremsstrahlung electrons, etc., in the lead of the apparatus. For this purpose, the ABCD hodoscope events were classified into two groups: (1) Events with one discharged counter in tray B, and one discharged counter in tray D ($B = 1$, $D = 1$). (2) Events with more than one counter discharged in either B or D, or in both. The events of the second group, which we shall call 'multiple events' can be classified according to the number of counters triggered in trays B and D. Table II gives a full and detailed analysis of the multiple events at various depths. All the multiple events can however be divided into three main categories:—

(i) one counter discharged in tray B and more than one counter discharged in tray D ($B = 1$, $D > 1$)

(ii) more than one counter discharged in tray B and one counter discharged in tray D ($B > 1$, $D = 1$)

(iii) more than one counter discharged in tray B and more than one counter discharged in tray D ($B > 1$, $D > 1$)

TABLE II

Complete and detailed analysis of the multiple events at various depths

Depth mwe	B=1, D=1 Singles	B=1, D=2						B=1, D=3			B=1, D=4	B=1, D=5	B=1, D=6	B=2, D=1						B=3, D=1				B=4, D=1	B=6, D=1	B=2, D=2	B=3, D=2	B=4, D=2	B=6, D=2	B=2, D=3	B=4, D=3	B=6, D=3	B=2 D=4	B=5, D=4	B=4, D=5	ABCD
		q = 0	1	2	3	4	Total	q = 0	1	Total				q = 0	1	2	3	4	Total	q = 0	1	2	Total													
10	503	11	2				13	1		1				18	2	1			21		2		2	1												541
22	449	7	1				8	1		1	1			9	3	1			13	1			1			1										474
503	167	12	2	1			15				1			14	1	3			18	2	1		3	1		1	1	1								208
598	236	17		1			18	3	1	4				15	2	1			18	5			5	1		1						2		2		287
807	156	13					13	5	1	6				9		1			10	2			2			2				2						191
1008	193	11	2			1	14	4		4	3	2	1	14	1				15	8	2		10	3	3	2	1			2	2	2	1	1		259

q stands for the number of undischarged counters intervening the discharged counters.

Table III gives the observed number of events falling into each of the various categories described above, and also the percentage values to facilitate comparison.

TABLE III

Classification of the hodoscope records, Arrangement I

Event \ Depth mwe	10 mwe	22 mwe	503 mwe	598 mwe	807 mwe	1008 mwe
ABCD	541	474	208	287	191	259
B=1 } D=1 }	503 93·0±4·1	449 94·7±4·5	167 80·3±6·2	236 82·3±5·4	156 81·7±6·5	193 74·5±5·4
B=1 } D>1 }	14 2·6	10 2·1	16 7·7	22 7·7	19 10·0	24 9·3
B>1 } D=1 }	24 4·4	14 3·0	22 10·6	24 8·4	12 6·3	31 12·0
B>1 } D>1 }	0 0	1 0·2	3 1·4	5 1·6	4 2·0	11 4·2
Multiple } Events }	38 7·0±1·1	25 5·3±1·3	41 19·7±3·1	51 17·7±2·5	35 18·3±3·1	66 25·5±3·1

Interpretation of the events

In the interpretation given below, the effect of the dead-space leakages of the counter geometry have been neglected. We assume that the leakage factor is the same at all depths, and regard the estimated percentages of multiple events as useful only for comparing the values at different depths.

1. *Events of the type* $B = 1$, $D = 1$.—These events are mostly due to:

   (*a*) single particles penetrating 10 cm. lead without producing secondaries;

   (*b*) single particles producing secondaries that pass through the same counters as the single particles;

   (*c*) two or more closely collimated penetrating particles passing through the same counters in B and D.

Without an exact knowledge of the angular distribution of the secondary particles, it is not possible to separate the contributions from the various groups. By regarding all the events of type $B = 1$, $D = 1$, as single particles, we obtain an upper limit to the number of single particles and a corresponding lower limit to the number of particles that are accompanied by secondaries.

2. (i) *Events of type* $B = 1$, $D > 1$.—Events of this type are caused by

(*a*) single penetrating particles producing secondaries in the 7·5 cm. lead between the trays C and D, the angles of emisison of the secondaries being sufficiently large for the secondaries, or the showers initiated by them to trigger neighbouring counters;

(*b*) two or more penetrating particles with angular separation such that they pass through the same counters in B and through different counters in D.

It is again difficult to separate the relative contributions of (*a*) and (*b*). Since it was observed that the events in which two neighbouring counters were discharged in both B and D were few [(in type (iii)], the contribution from the second type may be considered small compared to that from the first type (*a*). It is seen from Table III, that the percentage of these events increases from 2·6% at 10 mwe to 9·3% at 1008 mwe.

(ii) *Events of type* $B > 1$, $D = 1$.—These events are due to

(*a*) single penetrating particles incident on the telescope, accompanied by secondaries that can penetrate 2·5 cm. lead;

(*b*) single penetarting particles producing secondaries in 2·5 cm. lead plate, that cannot penetrate 7·5 cm. lead.

The upper limit to the contribution from the first type of events (*a*) was determined from a modified experimental arrangement (Arrangement II, as distinguished from the set-up of Fig. 1, which is Arrangement I) described in sub-section (B). From this, the lower limit to the percentage of particles that produced secondaries in the 2·5 cm. lead plate was known. Table IV gives the lower limits of percentages of secondaries produced in 2·5 cm. and in 7·5 cm. lead, for the three depths 22, 598 and 1008 mwe.

(iii) *Events of type* $B > 1$, $D > 1$.—These events are due to

(*a*) associated penetrating particles arriving from the rock;

(*b*) single particles producing penetrating secondaries in 2·5 cms. lead, with large angular separation;

(*c*) single particles producing secondaries in both the lead plates—double knock-on's, etc.

The total number of observed events of this type were small. The percentage increased from 0·2% at 22 mwe, to 4·5% at 1008 mwe.

TABLE IV

Secondary production in the lead of the apparatus and the rock

Description of event \ Depth (mwe)	10	22	503	598	807	1008
Percentage of particles which produce secondaries in 7·5 cm. lead block in the apparatus (lower limits)	2·6	2·1	7·7	7·7	10·0	9·3
Percentage of particles which produce secondaries in 2·5 cm. lead in the apparatus (lower limits)		2·8		5·8		8·9
Percentage of particles which produce secondaries in the lead of the apparatus (lower limits)		4·9		13·5		18·2
Percentage of events with particles coming as multiples from the rock, corrected (lower limits)		8·4		42·9		41·0

(*B*) *Secondary production in the rock*

To determine the percentage of particles that arrived at the telescope, accompanied by secondaries produced in the rock, the following modification was made in the experimental arrangement: The tray D which was below the 7·5 cm. lead block, was now placed above the tray A. The rest of the set-up remained the same. The counters in trays D and B were hodoscoped as before, with AC double coincidence pulse as the master pulse.

As in sub-section (A), the events were classified as follows:—

(i) *Events of type* $D = 1$, $B = 1$.—These events are due to

(*a*) single particles penetrating 2·5 cm. lead;

(*b*) closely collimated associated particles passing through the same counters in D and B;

(*c*) single particles producing secondaries in the 2·5 cm. lead plate, the secondaries passing through the same counter in D, as the primary.

By regarding all the events $D = 1$, $B = 1$, as due to single particles, we obtain a lower limit for the number of events with associated particles arriving from the rock. The percentage of the events $D = 1$, $B = 1$, decreases from 89% at 22 mwe, to 59% at 1008 mwe (Table V).

(ii) *Events of type* $D = 1$, $B > 1$.—These are due to

(*a*) single particles penetrating 2·5 cm. lead, producing secondaries that trigger the neighbouring counters in tray B;

(*b*) penetrating particles from the rock, which pass through the same counter in D, and through different counters in B.

It is seen from Table V, that the percentage of these events does not change appreciably with depth. These events could be caused by mesons as well as penetrating electrons.

TABLE V

Classification of the hodoscope events of Arrangement II

Level / Event	22 mwe	598 mwe	1008 mwe
DABC	548	310	203
D=1, B=1	485 88·5±4·0	184 59·4±4·4	120 59·1±5·4
D=1, B>1	33 6·0±1·1	29 9·4±1·8	16 7·9±2·0
D>1, B=1	28 5·1±1·0	84 26·9±2·9	52 25·6±3·6
D>1, B>1	2 0·4	13 4·3±1·2	15 7·4±1·9
Events with particles coming as multiples from top (D>1, B≧1)	30 5·5	97 31·2±3·2	67 33·0±4·0

(iii) *Events of type* $D > 1$, $B \geq 1$.—These events are due to particles which arrive as multiples from the rock. In this case, it was possible to get an estimate of the percentage of particles which were associated with secondaries that passed through the same counter as the primary particle. The calculation was made assuming a Gaussian distribution for the separation of particles, since the separation is governed mostly by scattering. From the frequency of events as a function of separation of the discharged counters, we calculated the constants of the distribution, and were able to get an estimate of the percentage of events in which closely collimated particles passed through the same counter. The corrected percentages of particles that arrived at the telescope as multiples for the three depths 22, 598 and 1008 mwe, are given in Table IV. It is found that

the percentage increases from 8% at 22 mwe to 42% at 1008 mwe. Comparison of these values with theoretical values is given in Section VII (C).

The events of the type $D > 1$, $B > 1$, in Arrangement II, were useful in finding the lower limit to the number of cases in which single penetrating particles produced secondaries in 2·5 cm. lead of the experimental arrangement I. Events of the type $D > 1$, $B > 1$, were those in which two or more particles came from the rock, each capable of penetrating 2·5 cm. lead, or one or both of them produced showers that triggered more than one counter in B. Therefore by regarding all events of the type $D > 1$, $B > 1$, as those in which two or more particles arrived from rock, with at least one of them capable of penetrating 10 cm. lead, we obtain an upper limit to the percentage of such events. This sets the lower limit to the percentage of cases in which secondaries were produced in the 2·5 cms. lead plate of arrangement I.

Section V. Deduction of the Energy Spectrum of π-Mesons and of μ-Mesons from Intensity Measurements Underground

If we make the assumption that μ-mesons are produced only as a result of the decay of π-mesons, then we normally expect the spectrum of μ-mesons to follow closely the energy spectrum of π-mesons at all energies, since the mass difference between π's and μ's is small. But at high energies the probability of absorption of π-mesons increases relative to the decay probability. This renders the μ-meson spectrum at the high energy end steeper than the spectrum of π-mesons in the corresponding energy range. If the differential energy spectrum of π-mesons at production is given by the power law $dN_\pi(E) = k \cdot E^{-r} dE$, and if we assume that the cross-section for the absorption of π-mesons is nuclear geometric upto the energies considered, then the μ-meson differential spectrum is given by (George, 1952; Greisen, 1948)

$$dN_\mu(E) = \frac{k \cdot E^{-r}}{1 + aE} \cdot dE$$

where $\frac{1}{a} = \frac{8 \times 10^5 \cdot m_\pi}{c\tau_\pi}$, m_π = rest energy of π-meson in Bev = 0·143 and τ_π = mean life-time of π-meson = $2 \cdot 4 \times 10^{-8}$ sec., and E is expressed in Bev. When π-mesons decay into μ-mesons the average energy of the μ-mesons is about 0·81 times the energy of the π-mesons. The integral energy spectrum of μ-mesons is therefore given by

$$N_\mu \ (> 0 \cdot 81\, E) = \int_E^\infty \frac{k \cdot E^{-r}}{1 + aE} \cdot dE \qquad (4)$$

To compare the experimentally determined intensities at various depths with the energy spectrum (4), we need the range-energy relation of μ-mesons. The range-energy relation of μ-mesons, considering the energy losses due to ionisation, bremsstrahlung, production of electron pairs, stars, penetrating particles, and Cerenkov radiation is given by (George, 1952)

$$R = \frac{2\cdot303\times10^{-2}}{b}\log_{10}\left(1+\frac{bE}{d}\right), \qquad (5)$$

where R and E are expressed in mwe and mev respectively. The constants b and d are determined by the mean atomic number Z and the mean atomic weight A of the material traversed. From the chemical composition of the rock underground (Hornblend Schist, sp.gr. 2·98), the mean value Z = 11, and A = 22, have been computed. These lead to the values $b = 5\cdot36\times10^{-6}$ gm.$^{-1}$cm.$^{+2}$, and $d = 2\cdot65$ Mev gm.$^{-1}$cm.$^{+2}$. From (5), the minimum energies of μ-mesons penetrating the various depths are calculated and given in Table I (column 2). The depths between 500 and 1008 mwe, roughly correspond to minimum μ-meson energies E_{min} between 150 and 400 Bev. The μ-meson integral spectrum (4) has been drawn in Fig. 6 on log-log scale (for the energy range $150 < E < 400$ Bev), for various

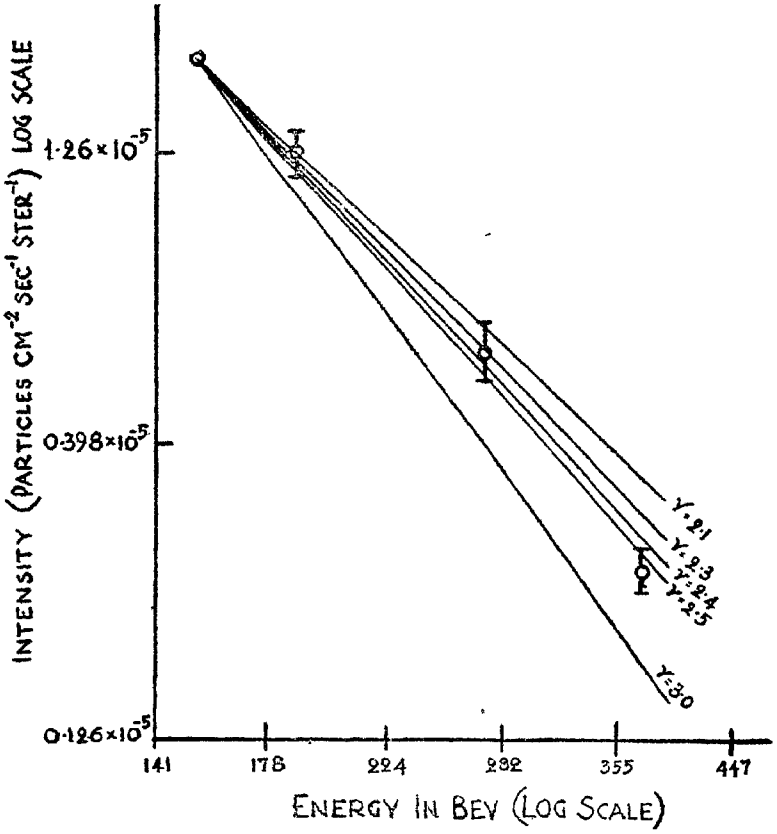

FIG. 6. Integral μ-Meson Energy Spectrum ($150 < E < 400$ Bev) for various values of γ—the exponent of the π-Meson Differential Spectrum.

values of γ, the exponent in the differential energy spectrum of π-mesons. Integration of (4) for non-integral values of γ is performed graphically. In the same figure, the experimental points obtained by us are also plotted. The curves have been normalised with respect to the 153 Bev experimental point (503 mwe). It is observed that the curves drawn with γ between 2·3 and 2·5 agree better than those with $\gamma = 2{\cdot}1$, or 3·0. The curve with $\gamma = 3{\cdot}0$ is much too steep and the one with $\gamma = 2{\cdot}1$ is much too flat to account for the observed experimental intensities. Therefore, a π-meson differential spectrum with the value of the exponent in the neighbourhood of 2·4, in the energy range $200 < E < 450$ Bev, fits best with our experimental results.

It is seen from Fig. 6, that the curves are not very different from straight lines. This means, that in the energy range under consideration ($150 < E < 400$ Bev), the integral spectrum of μ-mesons can be represented by a power law of the form $N_\mu (> E) = \text{constant}. E^{-\gamma}$. A least square fit for the first three experimental points gives the straight line

$$\log_{10} N_\mu (> E) = -0{\cdot}178 - 2{\cdot}09 \log_{10} E,$$

where N, the vertical flux is expressed in particles $\text{cm.}^{-2}\text{sec.}^{-1}\text{sterad}^{-1}$. This yields the power law for μ-meson integral spectrum

$$N_\mu (> E) = 0{\cdot}664\, E^{-2{\cdot}09 \pm 0{\cdot}02} \qquad (6)$$

in the energy range $150 < E < 300$ Bev. The least square fit for all the four points yields an exponent 2·41 instead of 2·09.

Section VI. Nature of Neutral Radiation Underground

The counting rates of the trays A, B, C and D, decreased by a factor five from 10 mwe, to 503 mwe, and remained practically the same at all lower depths. Coincidence experiments revealed that the contribution of charged particles to the tray counts was negligible, compared to that of the neutral radiation, converted in the counter walls. The efficiency of the counters for the detection of neutral radiation was obtained by determining the counting rate of a single counter, and the double coincidence rate of the single counter and a system of concentric ring of counters. The measured efficiency was about 1% and was the same as the efficiency of the counters for gamma rays, measured with a gamma source. The counting rate of a single counter was reduced only by 60% when it was shielded on all sides by 2·5 cm. lead. The energy of the gamma rays should be 2·5 mev, if 40% of the rays should be capable of penetrating 2·5 cm. lead. The radiation was found to be isotropic. The neutral radiation in the mines, is therefore essentially of radioactive origin.

SECTION VII. COMPARISON OF THE RESULTS WITH THE RESULTS OF OTHER EXPERIMENTS AND DISCUSSION

(*A*) *Intensity of cosmic rays at various depths*

Intensity measurements have been carried out previously by Wilson (1938) upto a depth of 1406 mwe, and by Clay and Gemert (1939) upto a depth of 1107 mwe. Wilson measured the total intensity with a four-fold coincidence single counter telescope, without any absorber between the counters. Clay and Gemert measured the intensity of penetrating radiation with a four-fold coincidence telescope of semi-angles 35° and 63°, and 10 cm. lead in the telescope. Total intensity was also measured by Miesowicz, *et al.* (1950), at depths 540 and 660 mwe. Miyazaki (1949), in Japan, measured the intensity of penetrating particles at depths 1400 and 3000 mwe. In order to compare our intensity measurements with those the above workers, we have calculated the vertical flux in terms of particles cm.$^{-2}$ sec.$^{-1}$ sterad^{-1} from the counting rates given by the various workers, assuming a cos^4 angular distribution for the particles at depths below 400 mwe. The calculated flux values of various workers are plotted in Fig. 7.

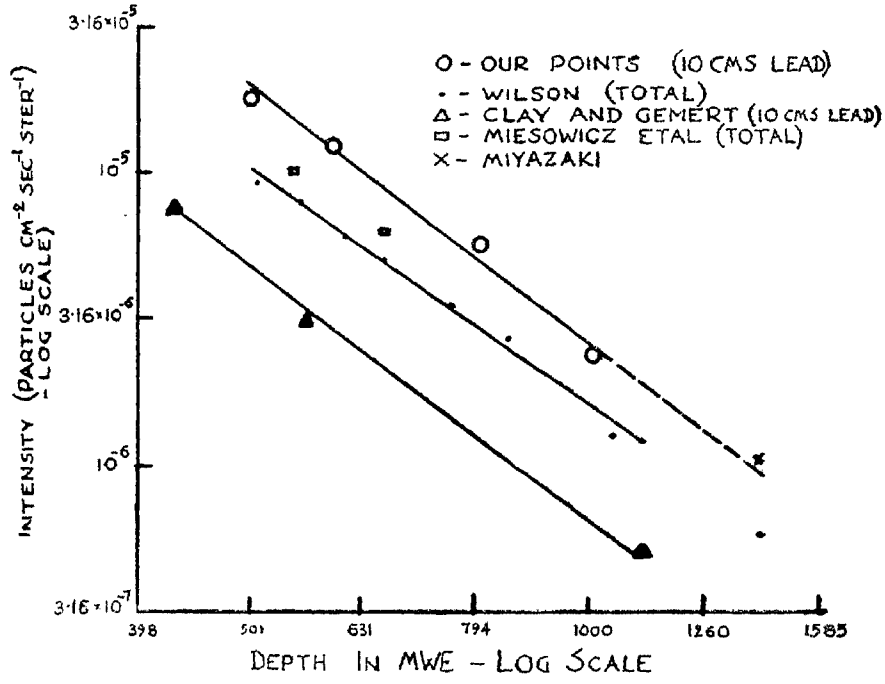

FIG. 7. Comparison of flux values of different workers.

It is seen that at all depths our flux values for the penetrating component are higher than the total intensity values of Wilson and Miesowicz,

et al., by a factor 2. Again our intensities for penetrating particles are higher than the corresponding intensities of Clay and Gemert by a factor 4·5. The flux value of Miyazaki for penetrating particles at 1400 mwe is twice the value of Wilson for total intensity at 1406 mwe. Extrapolating our curve to 1400 mwe shows that Miyazaki's flux value is consistent with our flux values obtained for depths 500–1008 mwe.

(B) Angular distribution of particles underground

Our measurements of the angular distribution give a $\cos^3$ variation at 22 mwe, and a $\cos^4$ variation at 598 mwe. Bollinger (1952) has measured the angular distribution of particles at 1600 mwe, with a hodoscoped counter telescope. His value for the cosine power is 3·1. As already stated, the total number of particles recorded by us is not quite sufficient to draw unambiguous conclusions regarding the exact power law obeyed by the underground particles.

(C) Secondary production by μ-mesons

At 22 mwe, about 5% of the mesons traversing the telescope produced secondaries such as knock-on's, bremsstrahlung electrons, etc., in the lead of our apparatus. The value increased to 18% at 1008 mwe (Table IV). These percentages are lower estimates, since the contribution from secondaries that pass through the same counters as the primaries could not be obtained. Tiffany and Hazen (1950) working with a cloud chamber at 860 mwe, have found a similar increase of secondary production. They found that at 860 mwe about 22% of μ-mesons traversing the chamber produced secondaries in the lead plates inside the chamber. Nassar and Hazen (1946) have found that the corresponding value at sea level is 6%. We can also compare the variation with depth, of the number of μ-mesons that are accompanied by secondaries, obtained in Section IV (B) (Table IV), with the theoretical prediction of Hayakawa and Tomonaga (1949). These authors have calculated the ratio of the number of electrons arriving at various depths accompanied by the generating mesons, to the total number of mesons at those depths. As explained in Section IV (B), our experiments give the percentage of mesons that arrive at various depths, accompanied by at least one secondary electron. The theoretical curve and the experimental points are plotted in Fig. 8. It is seen from the figure that the experimental values agree well with the theoretical values provided that mesons are accompanied mostly by single secondary electrons.

(D) Energy spectrum of π-mesons and of μ-mesons

In deducing the value of the exponent γ in the differential production spectrum of π-mesons, two assumptions were made:—(i) μ-Mesons are

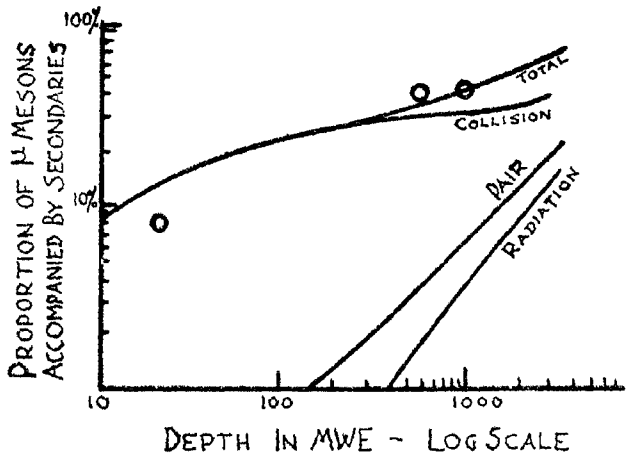

FIG. 8. Contribution of various processes (Collision, Pair production, and Radiation) to the equilibrium soft component at various depths.

produced only as a result of the decay of π-mesons; (ii) the cross-section for the absorption of π-mesons is nuclear geometric. It was reported at the Bristol Conference (December, 1951) by Perkins that at Bristol they had obtained evidence for the production of k-mesons along with the π-mesons, in high energy nuclear interactions, in the ratio $N_k/N_\pi = 0{\cdot}6 \pm 0{\cdot}2$. The average value of the mass of k-mesons given by them is $m_k = 1270\ m_e$. In a few cases they have identified the charged decay product of k-meson to be a μ-meson. If this result is established by further experiments, then our first assumption that μ-mesons result only as decay products of π-mesons is no longer tenable. It was shown in Section V that if we make the assumption that the μ-mesons observed underground are the decay products of π-mesons alone, then a π-meson production spectrum $dN_\pi\ (E) = k \cdot E^{-2{\cdot}4}$ reproduces the intensity-depth curve obtained by us. However, calculation shows that if we make the assumption that 50% of the mesons produced in nuclear interactions are k-mesons with a life-time $\leqslant 10^{-9}$ secs., then a much steeper production spectrum $dN_{\pi k}\ (E) = \text{constant} \cdot E^{-3{\cdot}0}$, will reproduce the observed intensity-depth curve.

Regarding the second assumption, it may be pointed out that the recent work of Lock and Yekutieli (1952) shows that the cross-section is nuclear geometric upto 1 Bev. Recent work in this Institute on production of stars in photographic emulsions by secondaries of penetrating showers, has revealed that the cross-section is of the same order (nuclear geometric) upto about 10^{12} ev. It seems therefore quite justifiable to assume the cross-section to be nuclear geometric for all energies considered by us.

SUMMARY

An investigation on cosmic-ray intensity was carried out in the Gold Mines at Kolar (Mysore State), with a hodoscoped counter telescope, upto a depth of 1008 mwe. The following conclusions may be drawn from the investigation:—

(1) The intensity-depth curves for particles penetrating 2·5 cm. lead, and for those penetrating 10 cm. lead, run parallel between 500 and 1008 mwe.

(2) The vertical intensity of penetrating particles in terms of particles $cm.^{-2}\,sec.^{-1}\,sterad^{-1}$ can be expressed by the power law $I_v = 10^{3.56} H^{-3.1 \pm 0.1}$ for $500 \leq H \leq 1008$ mwe.

(3) The flux values for the penetrating component obtained by us are higher than the flux values of the total component given by Wilson, by a factor 2, at all depths between 500 and 810 mwe. Our flux values for the penetrating component are higher than the corresponding flux values of Clay and Gemert by a factor 4·5. Our surface value of flux is in agreement with the surface values of Wilson, Clay and Gemert.

(4) The angular distribution follows approximately $\cos^3$ law at 22 mwe, and $\cos^4$ law at 598 mwe.

(5) The secondary production by μ-mesons in the lead of the apparatus, as well as the soft component that is in equilibrium with the hard component increases with depth. The experimental values giving the proportion of soft component that is in equilibrium with the penetrating component, agree well with the theoretical calculations of Hayakawa and Tomonaga.

(6) Assuming that all the μ-mesons observed underground are produced only as a result of the decay of π-mesons, the value of exponent in the differential spectrum of π-mesons at production in the energy range $200 < E < 450$ Bev, is found to be 2·4.

(7) The experimentally determined μ-meson integral spectrum in the energy range $150 < E < 300$ Bev is given by $N_\mu (> E) = 0{\cdot}664\, E^{-2.09 \pm 0.02}$.

(8) The neutral radiation underground is essentially of radioactive origin.

ACKNOWLEDGMENTS

We wish to express our gratitude to Dr. H. J. Bhabha, for suggesting the investigation, and for helpful discussions. We are highly indebted to Dr. Bernard Peters for the valuable advice given in preparing this paper,

It is a pleasure to thank Dr. R. Ramanna for the help given to us in starting this work at Kolar.

We wish to express our grateful thanks to Messrs. John Taylor and Sons, for according permission to carry out the experiments in the Mines at the Kolar Gold Fields. We are especially grateful to Mr. V. M. Sundararajan, and Mr. T. C. Barnett of Nundydroog Mines for taking a lively interest in the investigation and for providing us with all the necessary facilities underground.

APPENDIX

The hodoscope photographs enable us to obtain a rough indication concerning the angular distribution of the particles passing through the telescope. For this purpose, we consider events of arrangement II, in which one counter in tray D, and one in tray B were discharged. The six D counters are denoted by symbols D_1, D_2, $\cdots D_6$ and the six B counters by symbols B_1, B_2, $\cdots B_6$. The event in which the i-th counter of tray D, and the j-th counter of tray B are discharged is denoted by (D_iB_j).

(D_1B_1), (D_2B_2), $\cdots (D_6B_6)$, *i.e.*, events belonging to the group $i-j=0$, are caused by particles arriving within an angle of 16° on either side of the vertical direction, in the plane perpendicular to the counter axes. Similarly, events of the group $i-j=\pm 1$, are due to particles arriving within an angular interval $\theta_{min.}=0°$, and $\theta_{max.}=31°$ on either side of the vertical, the mean direction in the interval, θ_m being $15\frac{1}{2}°$. Similarly for $i-j=\pm 2$ $\theta_{min.}=15\frac{1}{2}°$, $\theta_{max.}=42\frac{1}{2}°$, and $\theta_m=29°$, and for $i-j=\pm 3$, $\theta_{min.}=29°$, $\theta_{max.}=51°$, and $\theta_m=40°$.

In certain cases, the angle defined by a single counter in D and a single counter in B, is only insufficiently covered by the tray C. Therefore not all the events $i-j=0, \pm 1, \pm 2, \pm 3$, are necessarily recorded as ABCD coincidences. Table VI gives the combinations (D_iB_j) in the four groups $i-j=0, \pm 1, \pm 2, \pm 3$, which are fully covered by tray C. The number of particles counted in these four angular intervals at 22 and 598 mwe are given in columns 5, 6 of Table VI.

For comparison, these numbers have to be normalised using the factors 5·5, 8, 6 and 2, which are equal to the numbers of possible combinations (D_iB_j) for the four groups $i-j=0, \pm 1, \pm 2, \pm 3$. There is yet another normalisation factor arising out of the fact that the centres of the counters in B are not equidistant from the centre of any particular counter in D and *vice versa*. These factors are the geometric factors for the conversion

TABLE VI

Angular distribution of particles at 22 and 598 mwe

Mean Angle θ_m	Group	Types of events in the group (D_iB_j)	No. of combinations (D_iB_j)	No. of events observed at 22 mwe	No. of events observed at 598 mwe	No. of events normalised at 22 mwe	No. of events normalised at 598 mwe
0°	$i-j=0$	(D_1B_1), (D_2B_2), (D_3B_3) (D_4B_4), (D_5B_5), (D_6B_6)	5·5*	132	59	183 ±17	82 ±10
15½°	$i-j=\pm1$	(D_6B_5), (D_5B_4), (D_4B_3), (D_3B_2) (D_1B_2), (D_2B_3), (D_3B_4), (D_4B_5)	8·0	164	65	164 ±13	65 ±8
29°	$i-j=\pm2$	(D_6B_4), (D_5B_3), (D_4B_2) (D_3B_5), (D_2B_4), (D_1B_3)	6	90	28	135 ±14	42 ±8
40°	$i-j=\pm3$	(D_6B_3), (D_1B_4),	2	12	7	63 ±18	37 ±14

* Only three-fourths of the angles defined by (D_1B_1) and (D_6B_6) are covered by tray C.

of the observed intensities in various angular intervals into absolute intensities (in particles cm.$^{-2}$ sec.$^{-1}$ sterad^{-1}) in the mean directions joining the centres of the counters. The normalised figures giving the relative numbers of particles in the four directions $\theta_m = 0°$, $15\frac{1}{2}°$, 29°, and 40°, for depths 22 mwe, and 598 mwe are given in columns 7, 8 of Table VI, and plotted in Figs. 4, 5.

REFERENCES

Bollinger, L. M. .. (See George, E. P., 1952).

Clay, J. and Gemert, A. .. *Physica*, 1939 *b*, **6**, 497.

Daniel, R. R., Davies, J. H., Mulvey, J. H. and Perkins, D. H. *Bristol Conference on V-Particles and Heavy Mesons* December, 1951).

George, E. P. .. *Progress in Cosmic Ray Physics*, Ch. VII, p. 395, Ed. by J. G. Wilson (North Holland Pub. Co., 1952).

Greisen, K. I. .. *Phys. Rev.*, 1948, **73**, 521.

Hayakawa, S. and Tomonaga, S. *Prog. Theor. Phys.*, 1949, **4**, 496.

Lock, W. O. and Yekutieli, G. .. *Phil. Mag.*, 1952, **43**, 231.

Miesowicz, *et al.* .. *Phys. Rev.*, 1950, **77**, 380.

Miyazaki, Y. .. *Ibid.*, 1949, **76**, 1733.

Nassar, S. and Hazen, W. E. .. *Ibid.*, 1946, **69**, 298.

Tiffany, O. L. and Hazen, W. E. .. *Ibid.*, 1950, **74**, 849.

Wilson, V. C. .. *Ibid.*, 1938, **53**, 337.